Beacon Splits in Air Traffic Control Radar Beacon System (ATCRBS)

NARAYAN P. MURARKA, Member, IEEE
PETER P. TOULIOS, Member, IEEE
DOMENICO LANERA, Member, IEEE
IIT Research Institute
Chicago, Ill. 60616

Abstract

The ATC radar beacon system is today's primary source of surveillance data for air traffic control. For en route traffic control, radar and beacon data are collected at numerous long range radar (LRR) facilities and typically sent by remote control to the air traffic control center (ARTCC) by a radar microwave link (RML). Self-supporting or guyed RML towers are installed at some LRR sites adjacent to the LRR antenna to establish a line-of-sight microwave path to the first repeater site. For these LRR sites, beacon splits and pulse-stretching effects have been observed particularly in the direction of the RML tower. This paper relates to the determination of the magnitude of the beacon split problem for such sites and the extent to which this problem is caused by the RML tower. It has been shown that the RML tower causes distortion in the patterns of both the directional and omnidirectional antenna. The nature and extent of these distortions are such that they tend to nullify the advantages achievable by the SLS and ISLS techniques. Consequently, the beacon split phenomenon may be referred to more specifically by the well-known "ring-around" effect. Finally, the paper makes a few recommendations for eliminating or reducing this problem.

Manuscript received July 29, 1974; revised June 16, 1975.

This work was supported by the Federal Aviation Administration, Washington, D.C., under Contract DOT-FA72WA-3082.

I. Problem Definition

Accurate and continuous knowledge of aircraft position is essential for the efficient function of the air traffic control (ATC) system. At present, the ATC radar beacon system (ATCRBS) fills this roll for both en route and terminal area traffic. For en route traffic, the basic surveillance information is gathered at the long range radar (LRR) facilities strategically located throughout the country. This information is then sent by remote control to the air route traffic control centers (ARTCC) by the Radar Microwave Link (RML). Self-supporting or guyed towers are generally installed adjacent to the LRR antenna to establish a line-of-sight microwave path to the first repeater site. At the ARTCC, the information is processed and displayed on a PPI for use by the air traffic controller. Under ideal conditions with no system or site related problems, a single return with a typical width of about 3° in azimuth is observed on the PPI scope for each aircraft in space. In practice, however, abnormalities are often observed on the PPI display which may appear in the form of either multiple, stretched, or broken returns. The overall problem is generically referred to as the beacon split phenomenon.

The characteristics of some of these abnormal returns are as follows. The multiple returns consist of several returns which are at about the same range but distributed over an extended azimuth interval with significantly different widths. Stretched returns, on the other hand, are continuous and stretched in azimuth over a 5° to 10° azimuth interval. In cases where such phenomena as sidelobe and reflected path interrogations can explain multiple and/or stretched returns, more specific terms such as ring-around or false targets are used to identify the problem. Another type of abnormal return is depicted by a discontinuity in the display of the otherwise normal single beacon return corresponding to one target in space. The position of this discontinuity or narrow gap is randomly distributed over the width of the return. This problem is called the broken target effect and is caused by missed interrogations.

This paper reports the results of an investigation of the beacon split problem observed at LRR sites where an RML tower is located near the LRR antenna. For such sites, beacon splits and pulse-stretching effects have been observed particularly in the direction of the RML tower. This paper relates to the determination of the magnitude of the problem, the extent to which the problem is caused by the RML tower, and the recommendations for corrective action. The problem is attacked by first determining both theoretically (Section IV) and experimentally (Section V) the nature and extent of the distortions in antenna patterns due to the presence of the nearby RML tower. Secondly, the paper determines the effect of pattern distortion on the operation of the ATCRBS (Section VI). Discussion then leads into the causes of beacon splits and possible corrective actions.

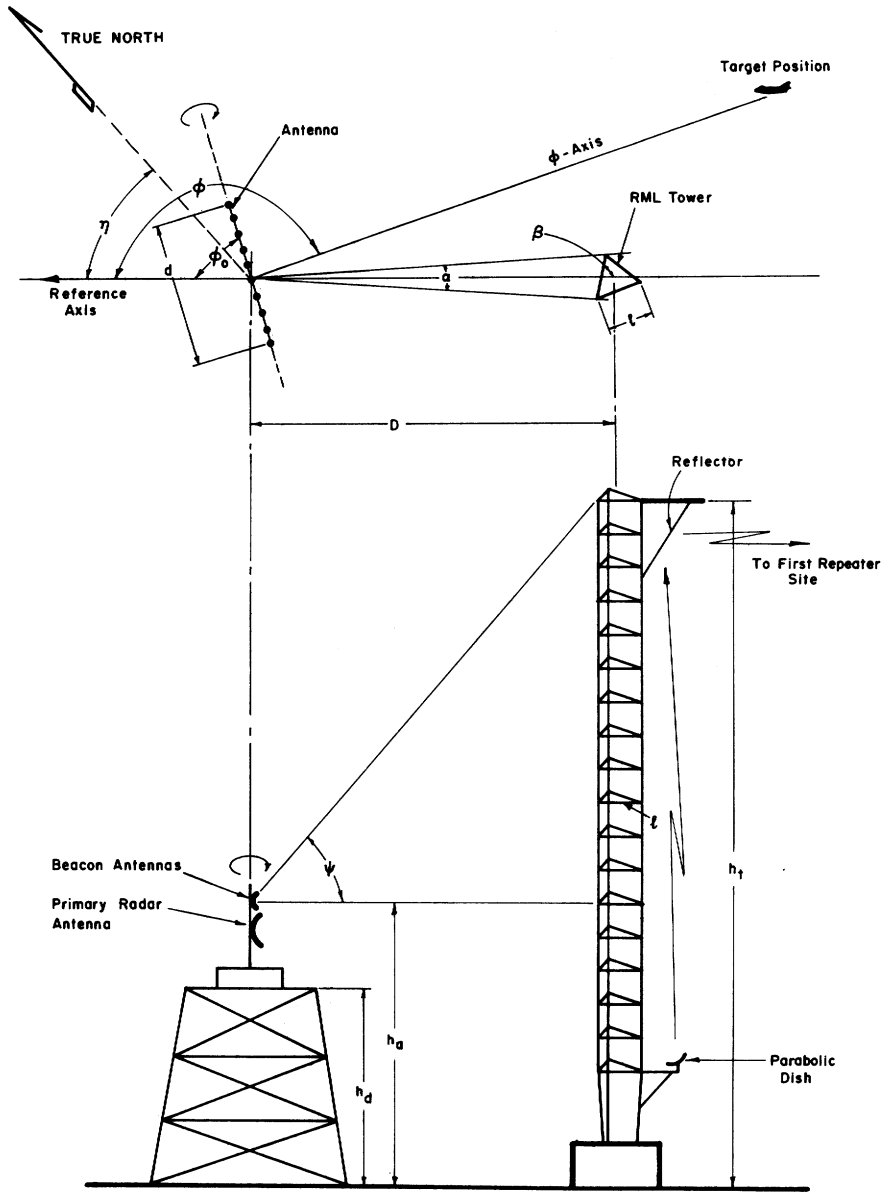

Fig. 1. Typical site layout.

II. System Details

The functional description of the ATC radar beacon system (ATCRBS) is given by Ashley et al. [1], Shaw et al. [2], and Drouihlet [3]. Recently, Marchand [4], [5] has also studied some related aspects of ATCRBS performance.

A typical LRR site geometry is shown in Fig. 1. An RML tower is located near the radar and beacon antenna mounted on a separate tower typically at a distance of 40 to 100 feet depending on the site. The height of the beacon antenna h_a varies from site to site but is typically 25 to 75 feet. The RML tower is triangular in cross section with each side being about 46 inches and its height can extend to about 200 feet. The target direction is indicated by an angle ϕ with respect to the reference axis shown in Fig. 1. The antenna orientation is given by the scan angle ϕ_0 formed by the reference axis and the line joining the antenna elements. Note that in defining the scan angle, the maximum of the main lobe is conventionally used instead of the line joining antenna elements as used here.

III. Summary of Available Data

An initial search for available data revealed that, except for one case, virtually no documented and systematic information was available about the nature and extent of the beacon split problem, although its existence was well recognized. The FAA southwest region conducted an evaluation and flight check of the split target problem at the Houston Intercontinental Airport (IAH) facility on October 15, 1969. They reported that the problem

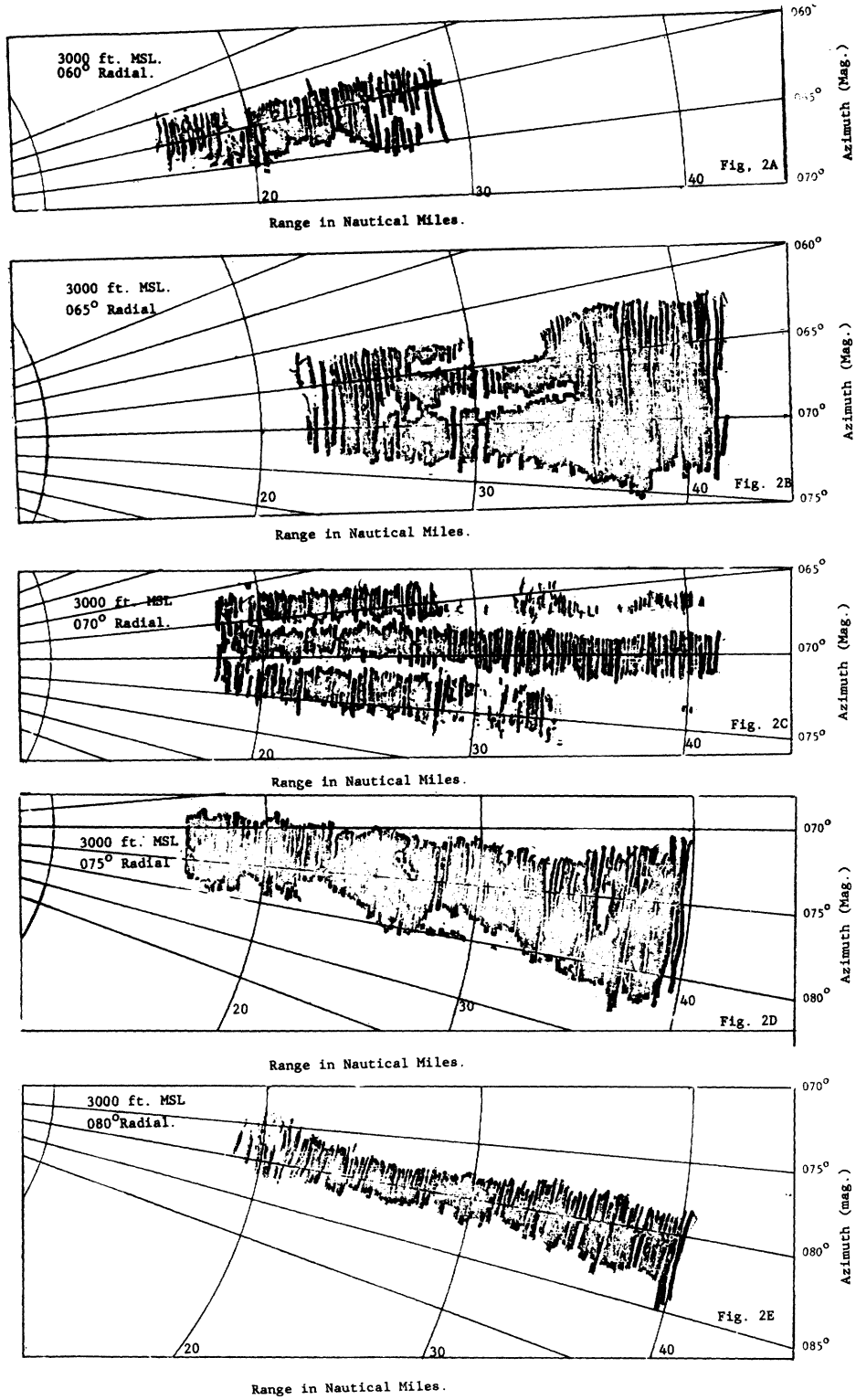

Fig. 2. Beacon returns obtained at Houston Intercontinental Airport (IAH).

occurred around the 70° radial which was directly in line with the tower.

Five flight tests were made between 20 and 40 miles from the site. Beacon targets were drawn as they appeared using grease pencil and a plastic overlay over the PPI scope. These target returns are reproduced in Fig. 2 for flights of an aircraft along five different radials.

On the 60° radial [Fig. 2(A)], targets are slightly stretched and some splitting is noticeable. On the 65° radial [Fig. 2(B)], targets are severely stretched, with some splitting around 30 miles. Stretching is toward the 70° radial which is in line with the RML tower. For the 70° radial [Fig. 2(C)] situation, three separate targets are generated over nearly the entire range. There is quite a bit of symmetry in this case. Along the 75° radial [Fig. 2(D)], targets are severely stretched toward the 70° radial again. Near-normal targets are observed for the 80° radial [Fig. 2(E)].

These flight results bring out the characteristics of beacon

splits along the direction of the RML tower. The authors reached similar conclusions about this problem at several other sites after careful study of time-lapse photographs of the PPI scope taken at these sites.

IV. Theoretical Analysis

An analytical model is used to derive the effect of the presence of an RML tower on the relative received power level at a transponder along a given axis ϕ as the directional antenna rotates. In the absence of an RML tower, the relative power level is obviously given by the antenna pattern. The model is also used to determine the distortion in the omniantenna (also called the SLS/ISLS antenna) pattern due to the RML tower. The model is represented by an infinite cylindrical tower illuminated by a linear array of 32 infinitely long dipoles with uniform distribution. The omniantenna case is treated by considering a single element instead of the 32-element array. This approximate model should show any pattern distortion in azimuth, but it is not general enough to give changes in the elevation plane. The model does not take ground reflection into consideration. The following discussion gives justification for using this simplified model.

The rotating directional beacon antenna used at the LRR sites is typically composed of a horizontal linear array of 32 elements with Chebychev amplitude distribution. It has a 3-dB bandwidth of about 2.35° in azimuth and about 36° in elevation. Considering the antenna vertical beamwidth, RML tower height, and the site geometry, it is apparent that the beacon antenna illuminates only a small portion of the tower. Consequently, the RML tower may be taken as an infinite vertical structure for analysis purposes. Further, the model views the individual elements as infinitely long current elements because the vertical pattern is not expected to be affected by the RML tower, since only a portion of it is illuminated [6, p. 237]. Finally, for the sake of simplicity, a 32-element linear array with uniform amplitude distribution is considered instead of Chebychev distribution. To keep the problem analytically tractable and yet realistic, the triangular RML tower is made equivalent to a cylindrical tower such that its circumference is equal to that of the triangular cross section. The radius of the cylindrical tower meeting this assumption is given by $a = 1.83$ feet.

A. Effects on Omniantenna Pattern

The presence of the RML tower causes the omniantenna pattern to be distorted. The pattern determined from the theoretical model (Fig. 3) shows different values of distance D between the antenna and RML tower. The primary effect is a drop in the power level in the direction of the tower, and this drop is spread over an azimuth interval ψ (hereafter called dip angle) around the direction of the RML tower. The significance of dip angle will be clear in Section VI which shows that the dip angle determines the azimuth interval over which the beacon-split phenomenon may occur. As shown in Fig. 3, the magnitudes of the drop in power level and the dip angle decrease as distance D increases. Fig. 4 summarizes this effect further with the target azimuth ϕ as a parameter. The secondary effect of the RML tower is to generate an oscillatory behavior in the antenna pattern as also shown in Fig. 3. It will be shown in Section VI that these distortions do not significantly contribute to the beacon-split phenomenon.

B. Effects on Directional Antenna Pattern

Under ideal conditions without the presence of the cylindrical tower in the near field of the directional antenna, the theoretical pattern of the model antenna is given by the dotted curve in Figs. 5 and 6. This curve also gives the fluctuation of the RF power at the transponder on an aircraft along a given azimuth ϕ as the scan angle ϕ_0 changes. In the presence of the RML tower, the relationship for the RF power level at the transponder is determined in the Appendix. The results are plotted in Figs. 5 and 6 with solid lines. These figures correspond to two different target azimuths, $\phi = 180°$ and $\phi = 178°$, respectively.

The primary effect of the RML tower on the RF power level is that the sidelobe levels increase, and the increment depends on the target azimuth angle ϕ. Further, there is an asymmetry in the increase in sidelobe levels. The magnitude of asymmetry depends on ϕ. When $\phi = 180°$, there is no asymmetry. However, for $\phi \neq 180°$ the increase in sidelobes 1A, 2A, etc., is different from that on sidelobes 1B, 2B, etc. The secondary effect is that the width of the main lobe and sidelobes also changes as shown in Figs. 5 and 6.

In order to study the effect of the RML tower on the ATCRBS performance, the combined effects of the omniantenna and directional antenna must be considered. It is particularly, necessary to know the net change of the sidelobe levels as compared to the distorted omni level. This can be obtained by combining the effects shown in Fig. 4 with those in either Fig. 5 or Fig. 6. The results are summarized in Fig. 7 for the first sidelobes 1A and 1B. Taking an example for the figure, the net changes in the levels of sidelobes 1A and 1B for a target flying along the $\phi = 178°$ axis will be about + 5.5 dB and + 3.1 dB, respectively, if the RML tower is located at $D = 40$ feet. For increased D, the net changes will be smaller. The effect of this net change on ATCRBS performance is considered in Section VI.

V. Experimental Verification

The system model used in the experimental investigation operated at 10.3 GHz (ten times the operating beacon frequency), thereby permitting 1/10 scaling of the physical sizes. A parabolic dish 4 feet in diameter and illuminated by a horn placed at its focus was used as a directional antenna with a 3-dB beamwidth at about 3° and with sidelobes at about 25 dB below the main lobe. Another horn with a 6-dB beamwidth of about 72° was used to simulate an omnidirectional antenna. A dipole could not be used as an

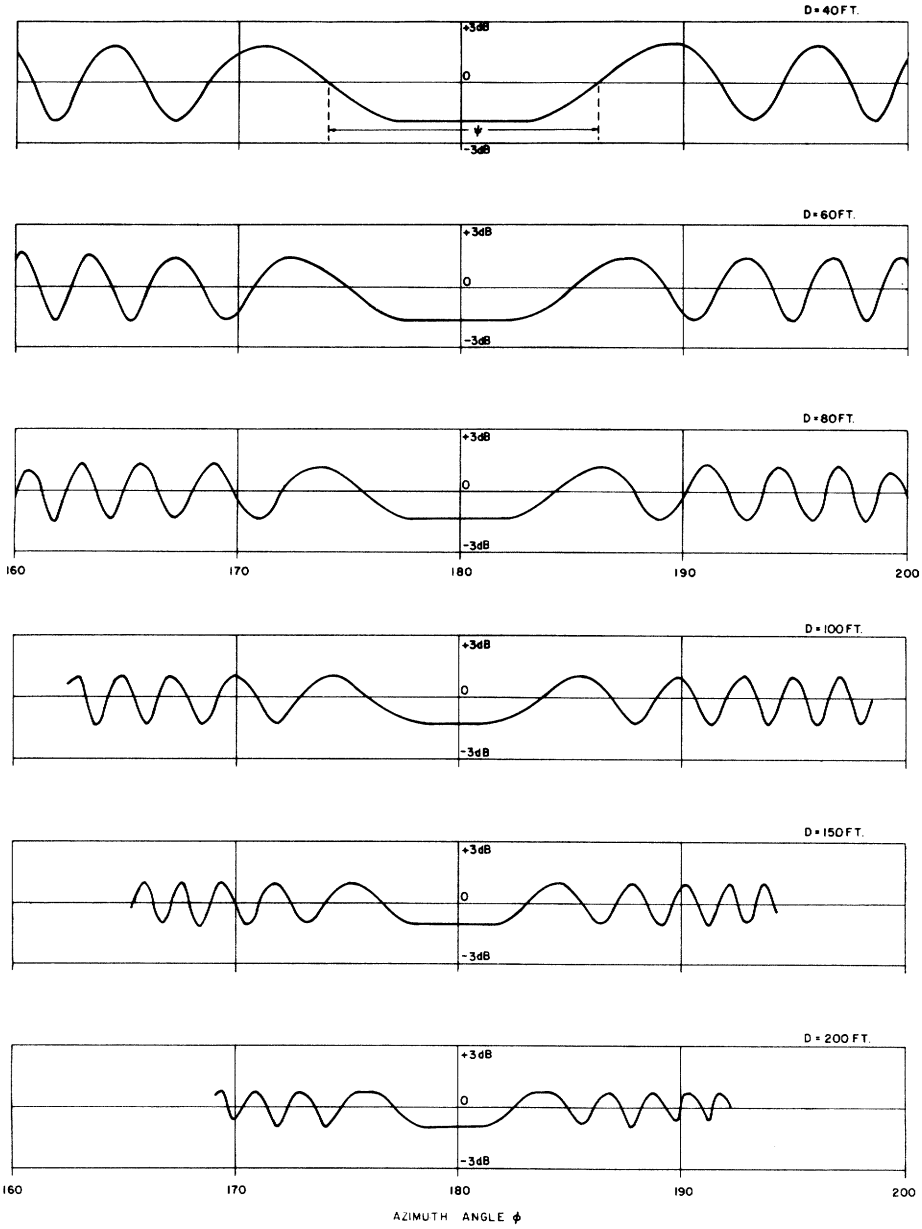

Fig. 3. Distorted omniantenna pattern (theoretical).

omniantenna due to reflection problems at the test site. However, this does not restrict the results since the nature and extent of wide beamwidth horn pattern distortion could be extrapolated to cover other azimuths.

A triangular structure with its three legs made of brass tubing of 3/8-inch diameter and supported by a number of braces was used as the model RML tower. The height of the tower was arbitrarily chosen as 6 feet such that it acted as a continuous structure to the vertical beamwidth of the model directional antenna.

A. Effects on Omniantenna Pattern

Using a standard antenna pattern test facility, the horn antenna patterns were obtained without and with the RML tower. These are shown in Figs. 8 and 9, respectively. Other patterns showed varying degrees of distortion when the RML tower was placed at different distances from the antenna. Examination of these patterns provided a qualitative confirmation of the conclusions obtained earlier from theoretical analysis. Quantitative differences between the theoretical and experimental results are apparently present, as could be expected due to slightly different models.

B. Effects on Directional Antenna Pattern

Fig. 10 shows the measured pattern of the model antenna in the absence of the RML tower and, therefore, also gives the relative power level at a transponder along $\phi = 180°$. Fig. 11 shows the results obtained by placing the RML

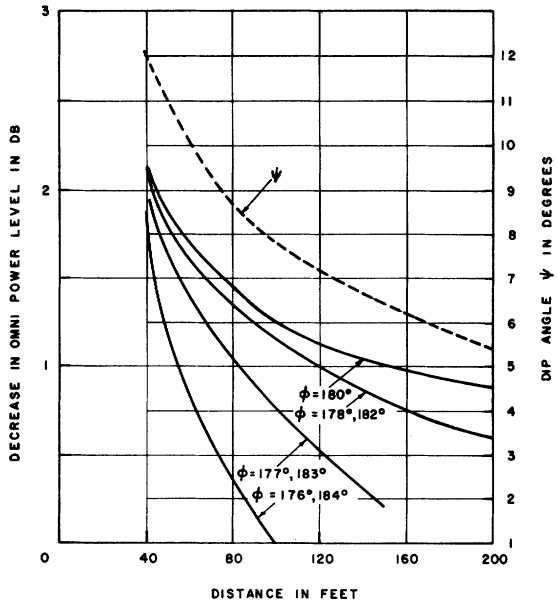

Fig. 4. Omniantenna distortion summary.

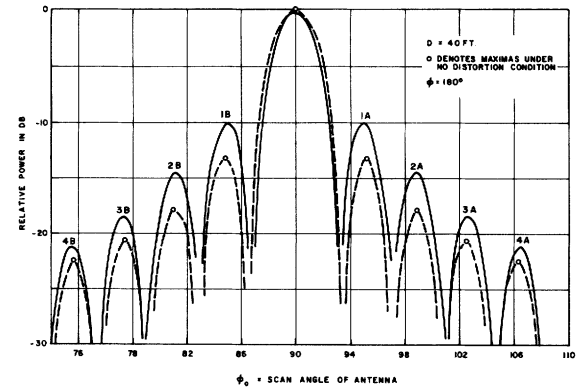

Fig. 5. Relative power at the transponder located at 180° azimuth.

Fig. 6. Relative power at the transponder located at 178° azimuth.

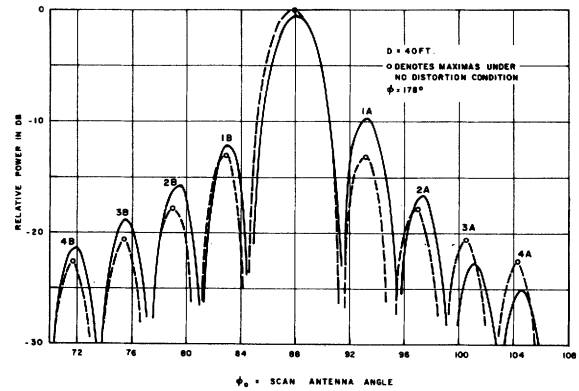

tower on a fixed platform in front of the parabolic dish. Examination of these and other figures verifies the outcome of the theoretical analysis from a qualitative point of view in that the antenna pattern changes significantly, particularly in terms of increased sidelobe levels and beamwidth. Quantitatively, however, a few discrepancies are noticeable, as could be expected, due to two different and simplified models used in the theoretical and experimental investigations.

VI. Causes of Beacon Splits

The causes of beacon splits will be apparent from an evaluation of the effectiveness of the sidelobe suppression (SLS) and improved sidelobe suppression (ISLS) techniques in the presence of antenna pattern distortions caused by the RML tower. It may be recalled that the SLS or ISLS techniques are used to inhibit the generation of reply pulses in response to sidelobe interrogations. This is achieved by a comparison between the power levels of the P1 (or P3) and P2 pulses received at the transponder. The P1 and P3 pulses are transmitted from the directional antenna, whereas the P2 pulse is transmitted from the omniantenna. Typical levels of the relative powers of these pulses at the transponder both under undistorted and distorted conditions are shown in Fig. 12 by dotted and solid lines, respectively. In Fig. 12 the P2 level is assumed to be 21 dB below that of the P1 (or P3) level. A threshold curve 9 dB above the P2 pulse power level is also drawn, and it intersects the P1 level curve at points A and B. According to SLS operation, the transponder is set to generate a reply whenever the P1 level is greater than the threshold level. Thus, while under no distortion, the width of the marker on the PPI scope will extend over an effective antenna beamwidth $\theta_1 \cong 4°$ as shown at the top of Fig. 12.

The relative power levels of the P1 and P2 pulses in the presence of the RML tower is also shown in Fig. 12 with solid lines. The P1 level distortion takes the form of increased sidelobe levels and wider beamwidths. P2 pulse power level distortion is shown by a drop near the RML tower azimuth and an oscillatory behavior in other azimuths. A new threshold curve is drawn 9 dB above that of the P2 level. As before, the transponder will generate replies whenever the P1 power level is greater than the threshold level. This occurs between azimuth intervals between the pairs of points E, F; G, H; and L, K for sidelobes 1A, 1B, and 2A, respectively. Due to assumed asymmetry in the pattern, there is no return for sidelobe 2B. The PPI display in this case shown at the top of Fig. 12 indicates that the beacon-split phenomenon occurs. The effects of the oscillatory pattern of the P2 level at other azimuth angles removed from the RML direction is negligible since the magnitudes of net distortion at these angles are not enough to cause replies from the transponder. The significance of the dip angle is also apparent in Fig. 12. It is over this azimuth interval that the beacon-split phenomenon is most significant.

The conditions under which the beacon-split phenomenon occurs can now be established quantitatively. With reference to Fig. 12, the various symbols are explained below:

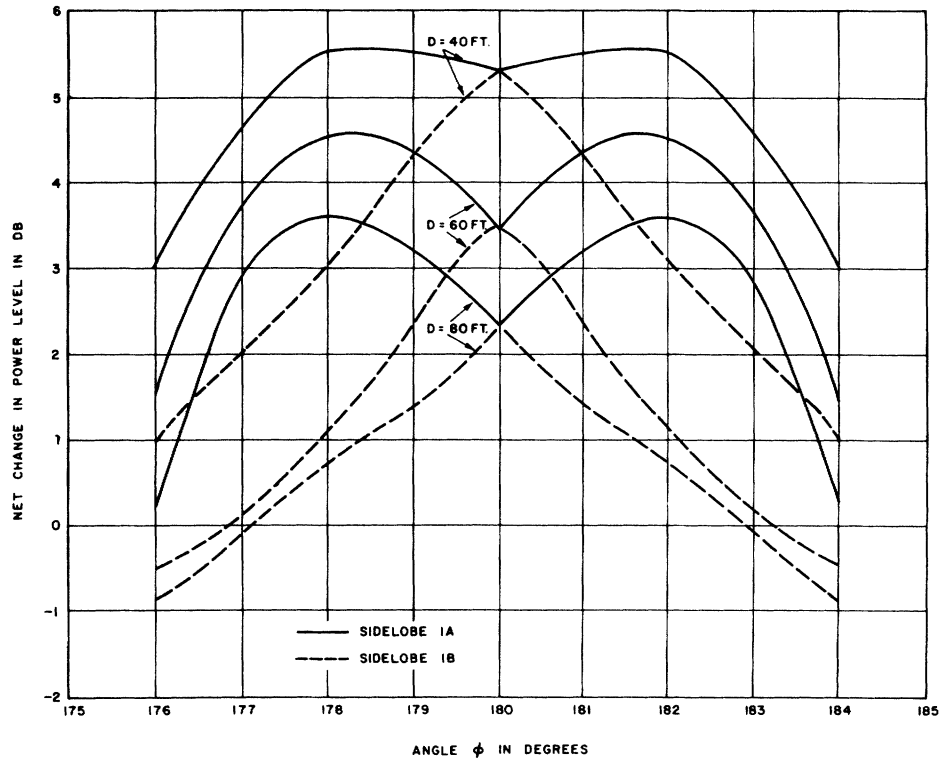

Fig. 7. Net change in power levels.

Fig. 8. Horn antenna pattern (undistorted).

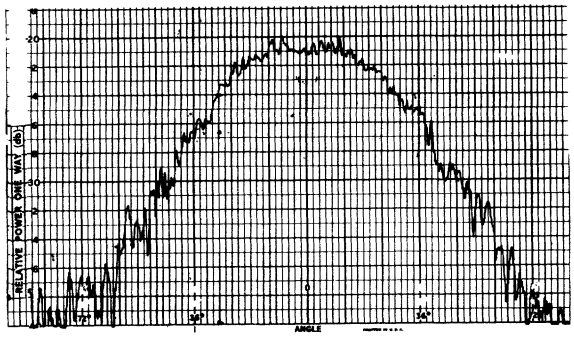

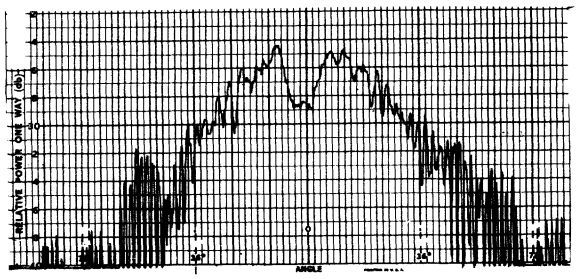

Fig. 9. Horn pattern with a metal tower on a revolving platform (D = 45 inches).

u = increase in sidelobe level of distorted pattern over that under undistorted condition in dB.

v = decrease in omniantenna power level of distorted pattern over that under undistorted condition in dB.

w = level of sidelobe level below omniantenna level under undistorted condition in dB. This is typically 7 dB as shown in Fig. 12.

q = net increase in sidelobe level over omnipower level under distorted conditions in dB.

t = threshold level used in the transponder.

The relationships between the above symbols are

$$\begin{aligned} q &= u - (w - v) \\ &= (u + v) - w \\ &= p - w \end{aligned}$$

where p can be interpreted as the net effect of the increased sidelobe level and decreased omni level and is the same as discussed earlier in Fig. 4. The condition for generating a reply at the transponder is satisfied when

$$q \geqslant t$$

or

$$p \geqslant t + w.$$

The value of w varies with the azimuth, and its minimum value is taken as 7 dB in this example. The U.S. standard

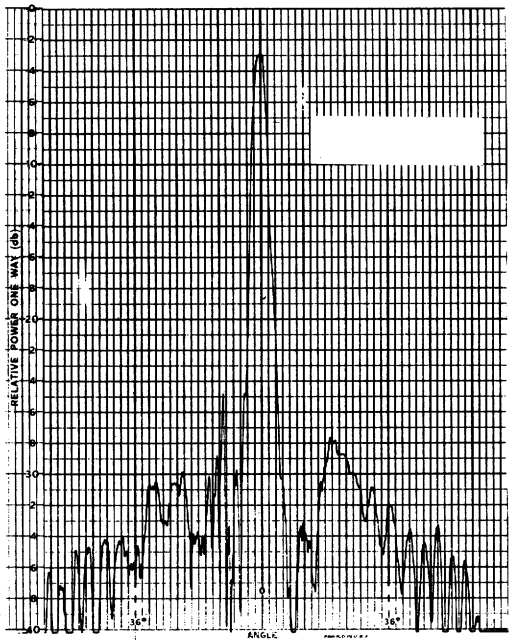

Fig. 10. Directional antenna pattern (undistorted).

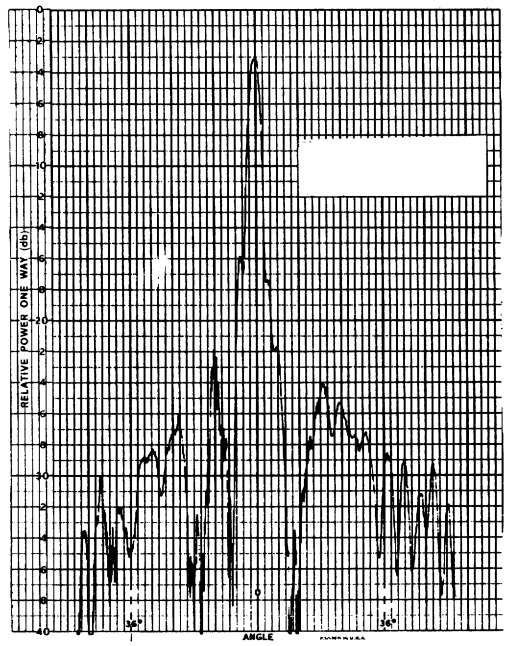

Fig. 11. Dish pattern with metal tower on fixed platform (D = 50 inches).

Fig. 12. SLS system power relationship under distorted condition.

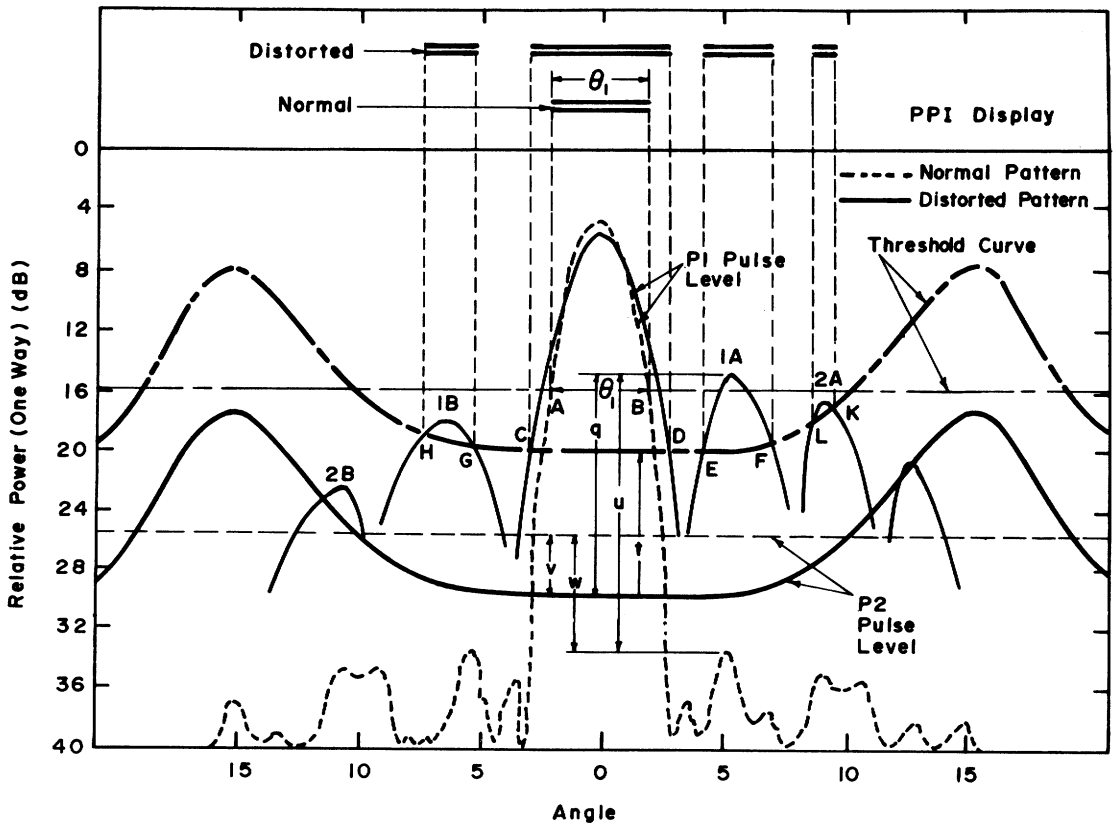

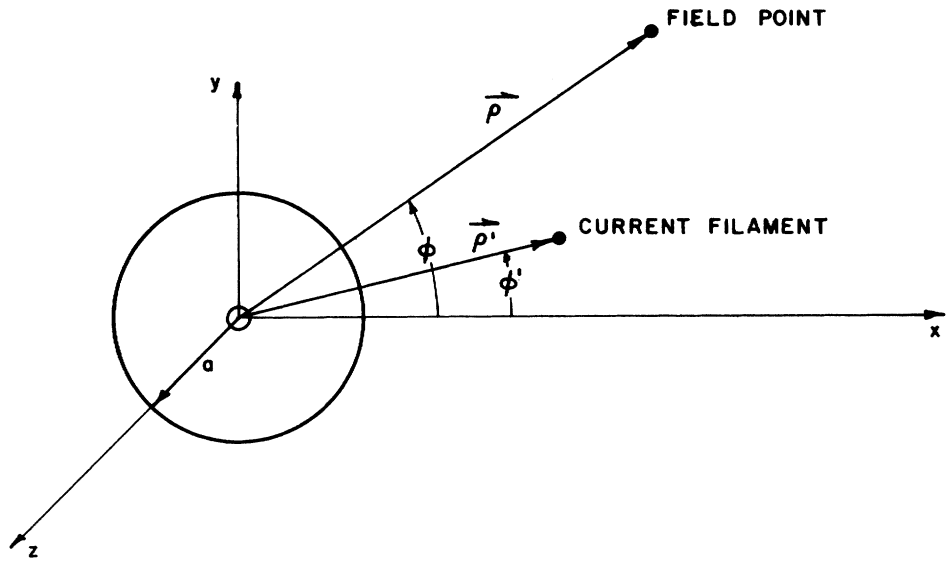

Fig. 13. A current filament parallel to a conducting cylinder.

for the threshold level is 9 dB which when adhered to will cause the beacon-split phenomenon to materialize whenever $p \geqslant 16$ dB. However, in the aviation industry considerable departure from this standard exists which adds a new dimension of randomness in the observation of beacon splits for different aircraft in the same environment. Such randomness was in fact found to exist during the observations of the PPI scope pictures.

It has been concluded that the RML tower contributes significantly to the beacon-split problem. This is due to the fact that the nature and extent of antenna pattern distortions due to proximity of the metallic RML tower tends to nullify the advantages achievable by the SLS technique. Similar considerations can be used to explain this problem at those sites which have ISLS capability. After knowing the causes of beacon splits, it is appropriate to use the more specific term *ring-around effect* to describe this problem. Other factors such as ground reflections may also contribute to the problem but have not been considered in this simplified analysis.

VII. Recommendations for Corrective Action

Relocation of the RML tower appears to be the most logical solution since it attacks the problem at its source. It should be moved beyond the far field boundary (about 1500 feet) of the directional antenna in order to completely eliminate its effect. However, a sufficient cure may be moving it only a few hundred feet where distortions are not sufficient to meet the condition ($p \geqslant 16$ dB) for beacon split. Such a distance has to be established from field tests. The relocation of the tower will require modifications of the microwave link path and establishment of an additional link (landline or microwave line of sight) between the radar site and the relocated RML tower. An alternative approach is to redesign the microwave link to completely do without the RML tower at the radar site.

Use of fiberglass materials for the RML tower also offers an alternative to the metal tower. Fiberglass towers have recently been found useful in other applications. Their characteristics should be extensively tested from electrical, mechanical, and structural points of view before reaching a final decision about their use in this application.

Appendix

I. Scattering by a Cylinder in Proximity to a Current Filament

As an intermediate step to solving the beacon-tower problem, it is essential to consider first the case of a current filament parallel to a conducting cylinder in order to calculate the far-field pattern of the omnidirectional antenna in the presence of the RML tower.

For a filament of electric current I, the incident field is given by (see Fig. 13 and [7, pp. 599-606])

$$E_z^i = -(k^2 I/4\omega\epsilon_0)\, H_0^{(2)}(k|\vec{\rho} - \vec{\rho}'|) \tag{1}$$

where

$k = 2\pi/\lambda$
$\omega = 2\pi f$
ϵ_0 = permittivity of free space
$H_0^{(2)}$ = Hankel function of the second kind and zero order.

For $\rho < \rho'$, by the addition theorem, (1) yields

$$E_z^i = (k^2 I/4\omega\epsilon_0) \sum_{n=-\infty}^{\infty} H_n^{(2)}(k\rho')\, J_n(k\rho) \exp[jn(\phi - \phi')] \tag{2}$$

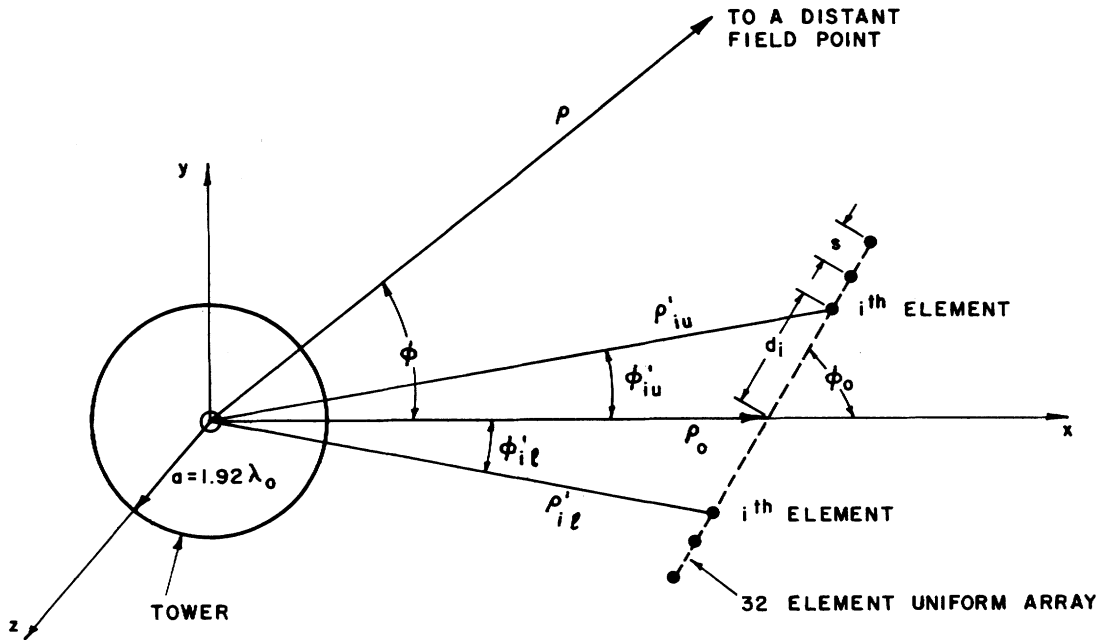

Fig. 14. Beacon antenna in proximity to a cylindrical tower.

where J_n = Bessel function of the first kind and nth order. The scattered field must be of the same form as (2), but with J_n replaced by $H_n^{(2)}$; namely,

$$E_z^s = (-k^2 I/4\omega\epsilon_0) \sum_{n=-\infty}^{\infty} C_n H_n^{(2)}(k\rho') H_n^{(2)}(k\rho) \cdot \exp\,[jn(\phi - \phi')]. \tag{3}$$

From (2) and (3) it is evident that

$$C_n = -J_n(ka)/H_n^{(2)}(ka) \tag{4}$$

satisfies the boundary condition

$$E_z = E_z^i + E_z^s = 0. \tag{5}$$

Thus, the final solution for $\rho > \rho'$ is

$$* \quad E_z = -(k^2 I/4\omega\epsilon_0) \sum_{n=-\infty}^{\infty} H_n^{(2)}(k\rho)\,[J_n(k\rho') + C_n H_n^{(2)}(k\rho')] \exp\,[jn(\phi - \phi')]. \tag{6}$$

Specializing (6) to the far zone (i.e., $\rho \to \infty$), one has

$$E_z = f(\rho)\{\exp\,[+jk\rho' \cos(\phi - \phi')] + \sum_{n=-\infty}^{\infty} j^n C_n H_n^{(2)}(k\rho') \exp\,[jn(\phi - \phi')]\} \tag{7}$$

where $f(\rho)$ is the amplitude constant for a given distance to the field point, and as such will be set equal to 1 in the following discussion. Note that $f(\rho)$ is proportional to the filament current I which will be the same for all elements of a uniformly excited beacon antenna. Equation (7) has been programmed for a digital computer and evaluated for typical field situations.

II. Formulation of the Beacon-Tower Problem

Having obtained the total radiated field due to a current filament in proximity to an infinite conducting cylinder, the solution to the beacon-tower problem becomes rather straightforward through superposition of contributions from the individual array elements. As explained in the introduction, the analytical model employed here is shown in Fig. 14. Note that the definitions for the symbols ϕ_0 and ϕ in Fig. 13 are slightly different from those used in Fig. 1. This was done for analytical convenience only and does not affect any results. Note that ϕ_0 is the scan angle of the beacon antenna array. Now let

E_{zi}^u = far field due to the ith element of the upper half of the array,
E_{zi}^l = far field due to the ith element of the lower half of the array.

Then the total far field due to beacon array is

$$E_z = \sum_{i=1}^{16} (E_{zi}^u + E_{zi}^l) \tag{8}$$

where, in accordance with (7),

$$E_{zi}^u = \exp\,[+jk\rho'_{iu} \cos(\phi - \phi'_{iu})] + \sum_{n=-\infty}^{\infty} j^n C_n H_n^{(2)}(k\rho'_{iu}) \cdot \exp\,[jn(\phi - \phi'_{iu})] \tag{9a}$$

$$E_{zi}^l = \exp\,[+jk\rho'_{il} \cos(\phi - \phi'_{il})] + \sum_{n=-\infty}^{\infty} j^n C_n (H_n^{(2)}(k\rho'_{il}) \cdot \exp\,[jn(\phi - \phi'_{il})], \tag{9b}$$

where

$$\rho'_{iu} = (\rho_0^2 + d_i^2 + 2\rho_0 d_i \cos\phi_0)^{1/2}, \tag{10a}$$

$$\rho'_{il} = (\rho_0^2 + d_i^2 - 2\rho_0 d_i \cos\phi_0)^{1/2}, \tag{10b}$$

$$\phi'_{iu} = \sin^{-1}(d_i \sin\phi_0/\rho'_{iu}), \tag{10c}$$

$$\phi'_{il} = \sin^{-1}(d_i \sin\phi_0/\rho'_{il}), \tag{10d}$$

$$d_i = (i - 1/2)\, s, \quad i = 1, 2, \cdots, 16, \tag{10e}$$

and

s = element spacing.

Equations (8) through (10) have been programmed for a digital computer and evaluated using the following parameters:

$ks = \pi$,
$\rho_0 = 40, 60, 80, 100, 150, 200$ feet,
$k\rho_0 = 256, 385, 513, 641, 960, 1282$,
$a = 1.83$ feet,
$ka = 12$.

The computer results have been discussed in Section IV.

Acknowledgment

Assistance provided by H. Bresler, J.A. Hilton, and R. Bishop of the Federal Aviation Administration, Washington, D.C., is gratefully appreciated.

References

[1] A. Ashley and J.S. Perry, "Beacons," in *Radar Handbook,* M. Skolnik, Ed. New York: McGraw-Hill, 1970, pp. 38.1-38.33.
[2] N.K. Shaw and A.A. Simolunas, "System capability of air traffic control radar beacon system," *Proc. IEEE*, vol. 58, pp. 399-407, 1970.
[3] R.R. Drouilhet, Jr., "The development of the ATC radar beacon system: past, present and future," *IEEE Trans. Communications Technology,* vol. COM-21, pp. 408-421, May 1973.
[4] N. Marchand, "Evanulation of lateral displacement of SLS antennas," *IEEE Trans. Antennas and Propagation,* pp. 546-550, July 1974.
[5] N. Marchand and D. Riva, "Laterally displaced ISLS antenna for tactical radar," *Navigation,* vol. 21, pp. 326-332, Winter 1974-75.
[6] R.F. Harrington, *Time-Harmonic Electromagnetic Fields.* New York: McGraw-Hill, 1961.
[7] E.C. Jordan, *Electromagnetic Waves and Radiating Systems.* New York: Prentice-Hall, 1958.

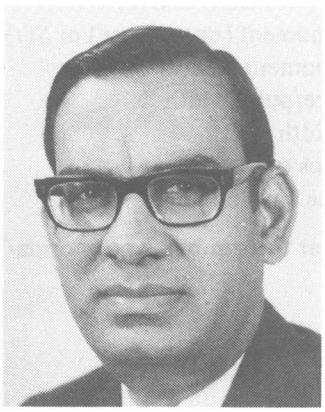

Narayan P. Murarka (M'64) was born in Calcutta, India, on Ocotber 7, 1938. He received the B.Sc. (Hons.) and M.Tech. degrees from the University of Calcutta, India, in 1959 and 1962, respectively, and the Ph.D. degree in electronic and electrical engineering from the University of Birmingham, England, in 1968. During his Ph.D. program and from 1968 to 1969, he was primarily engaged in research toward determining the characteristics of moon-reflected signals at *X* band. In this context, he was involved in the design of the experimental earth station and was successful in obtaining and analyzing moon echoes.

Dr. Murarka has been with IIT Research Institute, Chicago, since 1969, and his present position is Senior Engineer and Associate Manager. Here Dr. Murarka has been involved in a variety of projects in the areas of communications, air traffic control, navigation, and radar systems.

Dr. Murarka is a member of Sigma Xi and the Institute of Navigation. He also serves on several special committees of the Radio Technical Commission for Aeronautics (RTCA).

Peter P. Toulios (S'59–M'62) was born in Kastoria, Greece on January 16, 1934. He received the B.S. and M.S. degrees in electrical engineering from the University of Illinois, Urbana, in 1960 and 1961, respectively. He also received the Ph.D. degree in electrical engineering from the Illinois Institute of Technology, Chicago, in 1968.

In 1961 he joined IIT Research Institute, Chicago, where he worked on design and development of microwave components and antennas. He is currently with Epsilon Lambda Electronics Corp., Batavia, Ill., where he is involved in the design and development of microwave components and subsystems.

Dr. Toulios is a member of Sigma Xi and has served on various committees of the IEEE.

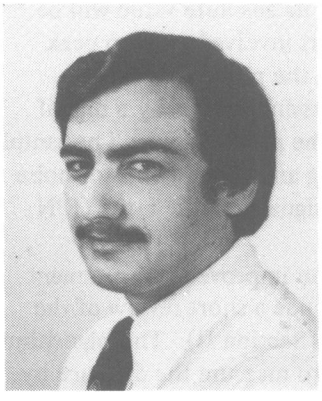

Domenico Lanera (M'71) was born in Italy on April 13, 1947. He received the B.S. degree in electronic engineering from the Illinois Institute of Technology, Chicago, in 1971.

He joined IIT Research Institute in 1972. Since that time he has been involved in various programs dealing primarily with air traffic control systems, radar analysis, EMP hardening, communication systems, and the development of computer softwares. His current interests are in computer modeling and anaylses, especially in the areas of air traffic, air navigation, and radars.

He is a member of Eta Kapp Nu and Tau Beta Pi.